RHIC ELECTRON-LENS BEAM PROFILE MONITORING*

T. A. Miller†, J. Aronson, D. M. Gassner , A. Pikin, C-AD, BNL, Upton, NY, 11973, U.S.A.

Abstract

In preparation for the installation of an Electron Lens [1] (E-Lens) into RHIC, planned for the summer of 2012, a test bench is being set up to allow the electron gun and collector assemblies to be tested together with a downsized mid-drift section. The goal of this effort is to test the electron gun and the collector designs, as well as the beam profiling instrumentation. A small unbiased Faraday cup, equipped with a grounded pin-hole mask, will intercept the beam; while an automated control and data acquisition system will raster scan the electron beam across the detector. A calibration procedure will allow the detection and compensation for offset & skew angles in both vertical & horizontal steering magnetic fields. The collected integrated charge measurement is digitized and stored in an image type data file. This pin-hole detector can be alternatively inserted in the same position as a YAG:Ce crystal. A viewing port at the downstream extremity of the collector allows a GigE camera, fitted with a custom zoom lens, to image the crystal and digitize the profile of a beam pulse. Custom beam imaging software is being written to provide the calibration and analysis of both beam image files (pin-hole and YAG) and fully characterize the image of the beam profile.

INTRODUCTION

The E-Lens test bench facility, located at the existing Electron Beam Ion Source (EBIS) test facility [3] at BNL, is nearly ready to see its first beam. As a complete overview of the diagnostics used was presented last year [3], presented here are design details and commissioning results of the beam profiling system. The goal of this system is to obtain a profile of the 5keV electron beam [4] from the gun by two independent methods and compare the results and to characterize the size and distribution of the resulting profile.

The first of the two methods captures an image of the electron beam on a scintillating YAG:Ce crystal using a digital camera and zoom lens mounted outside the vacuum chamber while peering through a viewport ~1.2m downstream of the YAG crystal, as depicted in Figure 1.

The second method raster scans the electron beam across a Faraday cup equipped with a 0.2mm pinhole mask. The collected charge is sent to remote integrating electronics mounted in an isolated rack floated at the potential of the collector (not more than 10kV to ground.) The integrator is triggered in synch with the 100Hz beam pulses. The DC output is digitized and stored in a data array along with the steering coil deflection set point as each position's coordinate.

* Work supported by B.S.A, LLC under contract No. DE-AC02-98CH10886 with the U.S. Department of Energy.
†tmiller@bnl.gov

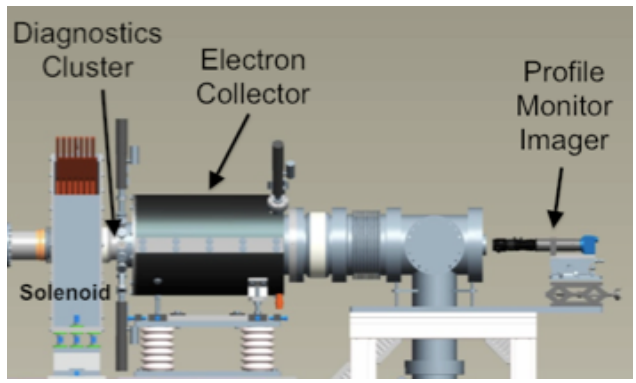

Figure 1: Downstream view of the collector on test bench showing Diagnostics Cluster (YAG & Pinhole elements), the Electron Collector, & the Camera & Zoom Lens.

YAG IMAGE ACQUISITION

YAG Crystal, Camera and Lens

Situated in the Diagnostics Cluster (Figure 1) is a 30mm YAG:Ce crystal, 0.1mm thick, made by Crytur [5]. It's held by an aluminum fixture that is actuated in & out by a pneumatic plunger. The first test will be made with a YAG crystal coated in house with 100nm of graphite to guard against charge build-up. To acquire images of the beam, scintillated in the YAG crystal, a monochrome digital camera with a 2/3" 1.2MP sensor (Sony ICX285) is used. This camera, model Manta G-145B, by AVT [7], employs a 14 bit ADC and a Gigabit Ethernet (GigE) digital communication interface allowing for up to 16 frames per second of full size images to be transferred over Ethernet. Although this camera employs a 14 bit ADC, the vendor comments that it's not practical to get better than 10 bits without actively cooling the sensor [6]. This camera very effectively heat sinks its sensor to its metal case but is not actively cooled.

In order to image the YAG crystal over the entire 2/3" sensor from so far away (1.2m), a custom zoom lens by Navitar was assembled. Although such a long zoom makes light scarce, it does an excellent job of ignoring large amounts of backscattered light from the illumination used during focusing & inspection.

Illumination

External illumination of the YAG crystal and holder is provided for periodic monitoring of proper lens focus and to check the health of the YAG crystal. Two sources of illumination were tested.

The first source was a prototype ring of 24 Ultra Bright White LEDs, model LEDWE-50, by Thor Labs [8], operating at their maximum current of 30mA. Installed around the end of the zoom lens, facing the large 4.0" viewport in the collector, this LED ring floods the collector with white light. Enough reaches the YAG

ISBN 978-3-95450-121-2

crystal & holder for a good image exposure, as seen in Figure 2a.

The second source was a single high power cold white collimated LED source, model MCWHL2-C1, from ThorLabs [8]. This source can focus its 410mW of white light onto a 3"x3" square 1.4m away, providing more than enough light for a good exposure.

Figure 2 compares the results of the two sources. The LED Ring brings out much detail; where a possible scratch on the crystal or in the coating can be seen. Although this defect is not evident with the collimated LED, this point source allows for a higher contrast view of the bezel around the YAG crystal, aiding in finding an optimum focus. Moreover, this later source is available in UV and is planned to be used in subsequent tests as a better in situ health check of the crystal. Its downside is the space required and an extra 1.5" of viewport radius.

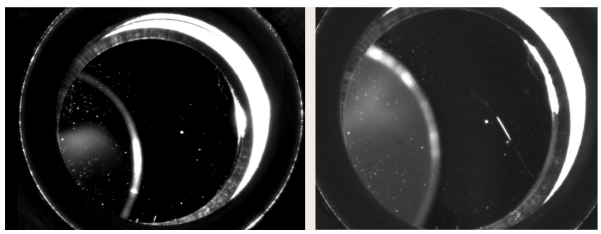

Figure 2: Illumination of YAG in holder.
a) *Left:* Collimated LED – high contrast bezel detail
b) *Right:* LED Ring – increased YAG surface detail

As the surface of the YAG crystal is polished to a mirror finish, the holder required a slight rotation of ~2º to avoid blinding the camera direct reflected illumination. This is evident in the views of Figure 2 as the partial view of the reflection of the downstream limiting aperture of the electron reflector [4].

Simulations with UV Laser

In an attempt to simulate the effect of an electron beam on the YAG crystal, a 405nm laser (5mW laser pointer) was used to excite the crystal in a local spot (~2x4mm). This helped detect non-uniformities in the YAG crystal. Figure 3 shows images captured of the laser exciting the YAG crystal. As the camera is sensitive to UV a 435nm long pass filter, model FGL435S, from ThorLabs [8], was placed in front of the camera to block back scattered UV.

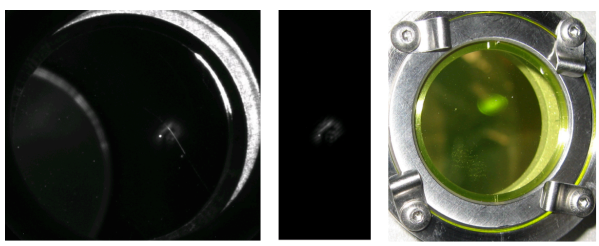

Figure 3: 405nm UV laser spot on YAG crystal in situ.
a) *Left:* UV laser on YAG with LED Ring illumination,
b) *Middle:* UV laser on YAG without illumination,
c) *Right:* UV laser on illuminated YAG (bench test)

In the Figures 3a & 3b, the UV laser was aimed at the apparent scratch showed by the LED ring illumination. However, without the LED illumination the UV laser doesn't show this scratch. Thus, the scratch must not be in the YAG crystal, but perhaps only in the graphite coating.

PINHOLE SCAN ACQUISITION

Automatic sequencing code runs in a frontend computer (FEC) in a VME crate and controls a RHIC V202 multichannel delay module, configured as a function generator (or sequencer). The code takes a file loaded with raster scan setpoints for the horizontal (H) and vertical (V) steering coils and synchronizes the firing of the electron beam and triggering of all instrumentation, especially the integrator connected to the pinhole Faraday cup. As the beam is scanned through the array of points, the beam intensity is sampled through the 0.2mm pinhole aperture. The system saves the digitized output from the integrator as a point in an array having the coordinates of the H & V scan setpoints (see Fig. 6a). The intent is for this file to map the distribution of the beam intensity. Finally a comparison is made of this map to that contained within the YAG image in hopes of a confirmation. But before this comparison can be made, the coordinates of the pinhole data array points must be calibrated to match their counterparts in the YAG image from the camera.

Calibration

In order to begin comparing the pinhole data to the YAG image data, a common ground must be established. By creating a Reference Circle (see Fig. 4) in a custom designed image analysis program and overlaying it on a camera image of the YAG crystal (of known diameter) we can establish a coefficient K_1 in mm/pixel.

$$K_1 = \frac{YAGCirDia_{mm}}{refCirDia_{px}} \quad (1)$$

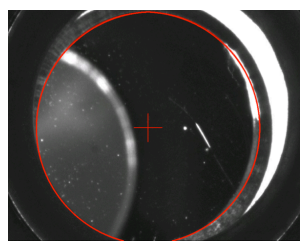

Figure 4: Reference circle overlaid on camera image of YAG crystal of known diameter.

A coefficient is calculated relating the steering coil setpoints in Amps (X, Y coordinates in the data array) to the deflection as observed by the camera in pixels. Thus, for the V axis coefficient, an image must be taken of the YAG with a beam pulse at its max. & min. vertical deflection limits. The program measures the vertical distance between the two beam centers as $\Delta Deflection_{px}$.

ISBN 978-3-95450-121-2

Comparing this distance to that of the Vertical deflection setpoint, $\Delta Setpoint_{Amps}$ (Y_1-Y_2), in Amps, we establish a "gain" coefficient K_V in pixels/Amps.

$$K_V = \frac{\Delta Deflection_{px}}{\Delta Setpoint_A} \quad (2)$$

The coefficient K_H is calculated in the same manner as above. Further calibration is necessary to compensate for possible offsets and coupling of the steering coils. Therefore, the two images are overlaid in the image analysis program and center markers are automatically applied to each and a line drawn between their centers. The program measures the offset of the center of the line with respect to the center of the Reference Circle and the angle the line makes to the image vertical axis. The same procedure is repeated for the H axis.

Examples of both are shown in an exaggerated example in Fig. 5; where the Vertical axis error (α) is -10º with an offset Y_0 = +48 pixels and the Horizontal axis error (β) is +10º with an offset of X_0 = +31 pixels.

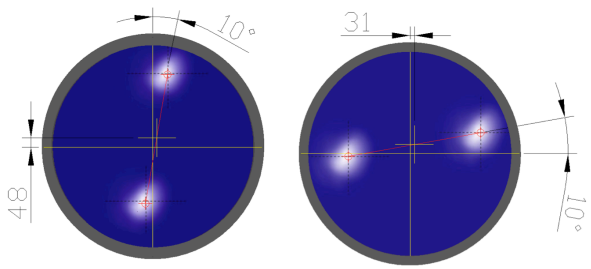

Figure 5: Offset and angle error measurements.
a) *Left:* Vertical axis steering coil error
b) *Right:* Horizontal axis steering coil error

To warp the perfect coordinate space to have the measured coupling, the transformations in (3) are made. See results of the exaggerated example in Figure 6.

$$\begin{aligned} X' &= X\cos(\beta) - Y\sin(\alpha) \\ Y' &= X\sin(\beta) + Y\cos(\alpha) \end{aligned} \quad (3)$$

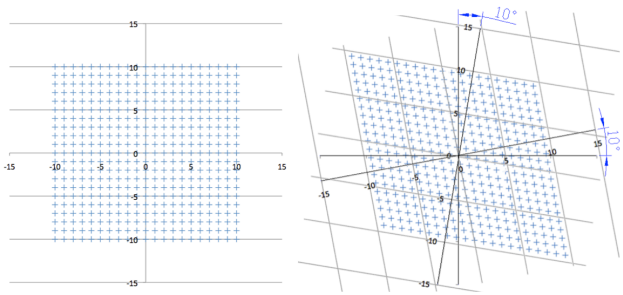

Figure 6: Axis rotation – exaggerated for clarity
a) *Left:* Example of non-rotated data coordinate space
b) *Right:* Example of rotated axes with different angles

The setpoint coordinates (X_n, Y_n) must be transformed from Amps to pixels using the coefficients K_V & K_H found in (2). The H & V offsets X_0 and Y_0 (in pixels) are added. The resulting expression (in pixels) is modified by the gain term K_1 found in (1) to convert all pixels to millimeters. Thus a final transformation of the array of raster scan setpoint coordinates (not the magnitudes) in the pinhole data file is made by replacing each of the coordinates (X,Y) with the transformed coordinates (X',Y'), as obtained from the combined expressions in (4) for coupling, offset and gain.

$$\begin{aligned} X' &= K_1\left[K_H\left(X\cos(\beta) - Y\sin(\alpha)\right) + X_0\right] \\ Y' &= K_1\left[K_Y\left(X\sin(\beta) + Y\cos(\alpha)\right) + Y_0\right] \end{aligned} \quad (4)$$

The image analysis program imports the modified pinhole data file for comparison of its beam profile to that contained within the image file from the YAG camera. The hope is to prove that the YAG camera image contains accurate enough data to rely solely on it for periodic beam profile measurements.

STATUS AND SCHEDULE

The first electron beams on the test bench are expected around mid April 2012. The E-Lens project schedule remains on track with installation of two complete E-Lens systems in the RHIC tunnel (one for blue and one for yellow beams), each equipped with the beam profiling system described herein, in the summer of 2012.

ACKNOWLEDGEMENTS

The authors would like to thank Matthew Stetski for groundwork done during the summer of 2011 on the image analysis program, as well as A. Bzdac, J. Hock, K. Hamdi, C. Liu, X. Gu and members of the controls group, especially A. Fatma, A. Fernando, L. Hoff, R. Olsen, & C. Theisen, and recognize the support of the Accelerator Components & Instrumentation Group, especially N. Baer, J. Carlson, T. Curcio, B. Johnson, J. Kelly, D. Lehn, J. Siano, D. Von Lintig, & A. Weston.

REFERENCES

[1] W. Fischer, Y. Luo, et al, "Status of the RHIC Head-On Beam-Beam Compensation Project", IPAC10, Kyoto, Japan, MOPEC026, p. 513.
[2] D. Gassner, et al, "RHIC Electron Lens Test Bench Diagnostics", DIPAC 2011, Hamburg, Germany, MOPD04, p. 38; JACoW, https://www.jacow.org
[3] E. Beebe, J. Alessi, S. Bellavia, et al, "Results of Beam Tests on a High Current EBIS Test Stand", PAC '99, New York, WEA9, p. 1902; JACoW, https://ww.JACoW.org.
[4] A. Pikin, et al, "Structure and Design of the Electron Lens for RHIC", PAC '11, New York THP100, p. 2309; JACow, https://www.jacow.org
[5] Crytur Ltd., https://www.crytur.cz
[6] Tom Hospod private communication. 1st Vision, Inc. technical sales. https://www.1stvision.com
[7] Allied Vision Technologies, https://www.alliedvisiontec.com
[8] ThorLabs, https://www.thorlabs.com

ISBN 978-3-95450-121-2